MOLECULAR AND CELLULAR BIOLOGY, Aug. 2000, p. 5454–5468 Vol. 20, No. 15
0270-7306/00/$04.00+0

BNIP3 and Genetic Control of Necrosis-Like Cell Death through the Mitochondrial Permeability Transition Pore

C. VANDE VELDE,[1] J. CIZEAU,[1] D. DUBIK,[1] J. ALIMONTI,[1] T. BROWN,[1] S. ISRAELS,[1] R. HAKEM,[2] AND A. H. GREENBERG[1]*

The Manitoba Institute of Cell Biology, University of Manitoba, Winnipeg, Manitoba R3E 0V9,[1] and The Amgen Institute, Ontario Cancer Institute, University of Toronto, Toronto, Ontario M5G 2C1,[2] Canada

Received 7 January 2000/Returned for modification 22 February 2000/Accepted 3 May 2000

Many apoptotic signaling pathways are directed to mitochondria, where they initiate the release of apoptogenic proteins and open the proposed mitochondrial permeability transition (PT) pore that ultimately results in the activation of the caspase proteases responsible for cell disassembly. BNIP3 (formerly NIP3) is a member of the Bcl-2 family that is expressed in mitochondria and induces apoptosis without a functional BH3 domain. We report that endogenous BNIP3 is loosely associated with mitochondrial membrane in normal tissue but fully integrates into the mitochondrial outer membrane with the N terminus in the cytoplasm and the C terminus in the membrane during induction of cell death. Surprisingly, BNIP3-mediated cell death is independent of Apaf-1, caspase activation, cytochrome *c* release, and nuclear translocation of apoptosis-inducing factor. However, cells transfected with BNIP3 exhibit early plasma membrane permeability, mitochondrial damage, extensive cytoplasmic vacuolation, and mitochondrial autophagy, yielding a morphotype that is typical of necrosis. These changes were accompanied by rapid and profound mitochondrial dysfunction characterized by opening of the mitochondrial PT pore, proton electrochemical gradient ($\Delta\psi m$) suppression, and increased reactive oxygen species production. The PT pore inhibitors cyclosporin A and bongkrekic acid blocked mitochondrial dysregulation and cell death. We propose that *BNIP3* is a gene that mediates a necrosis-like cell death through PT pore opening and mitochondrial dysfunction.

Kerr et al. (22), on the basis of distinct morphological criteria, identified apoptosis as a programmed and intrinsic cell death pathway, in contrast to necrosis, which was viewed as a passive response to injury. It is now clear that apoptosis is a highly regulated genetic program that is evolutionarily conserved in multicellular organisms and is essential for development and tissue homeostasis (19, 57). The genetic program results in the activation of cysteine aspartyl proteases (caspases) that cleave nuclear and cytoplasmic substrates and disassemble the cell (11, 54), yielding the characteristic morphological features such as chromatin condensation, DNA fragmentation, plasma membrane blebbing, and the formation of apoptotic bodies (58). In contrast to apoptosis, necrosis is considered an unregulated process occurring in response to toxicants and physical injury. This form of cell death is morphologically characterized by extensive mitochondrial swelling, cytoplasmic vacuolation, and early plasma membrane permeability without major nuclear damage (22, 23, 55).

Mitochondria appear to play a central role in the induction of cell death. This is thought to occur by at least three possible mechanisms: (i) release of apoptogenic proteins that facilitate caspase activation, (ii) disruption of electron transport, oxidative phosphorylation, and ATP production that may result in an energetic catastrophe, and (iii) alteration of the redox potential, resulting in increased cellular oxidative stress (14). The main biochemical determinant of apoptosis is the activation of caspases, and this is in part regulated by mitochondria. All caspases are synthesized as an inactive polypeptide (zymogen) that must be proteolytically processed to form an active tetramer (11). Recent work proposes that this processing is initiated through autocatalytic activation. For example, the caspase 8 zymogen is aggregated for autoprocessing by ligand-induced clustering of trimeric death receptors such as CD95/Fas (48). Active caspase 8 cleaves the proapoptotic BCL-2 family member BID, which is then able to translocate to mitochondria (30, 32). BID, as well as many other apoptotic signals, induces mitochondria to release cytochrome *c*, which functions as a cofactor with dATP for Apaf-1 binding and activation of caspase 9 and downstream effector caspases (31, 51). Another less well studied mitochondrial apoptogenic protein is apoptosis-inducing factor (AIF), a flavoprotein released in response to apoptotic signals that translocates to the nucleus to induce DNA fragmentation and chromatin condensation in a caspase-independent manner (53).

Apoptotic cell death signals induce other mitochondrial changes, such as opening of the permeability transition (PT) pore, a putative highly regulated ion channel located at the contact sites between the inner and outer mitochondrial membrane (8). The PT pore is a large protein complex, primarily composed of the adenine nucleotide transporter (ANT), cyclophilin D, and voltage-dependent anion channel (VDAC [also called porin]), that can interact with several other proteins (8, 25). When the PT pore is in the open state, it permits the passage of solutes of ~1,500 Da and results in depolarization of mitochondria, which consequently decreases the measured proton electrochemical gradient ($\Delta\psi m$). This, in turn, can lead to the inhibition of respiration, generation of reactive oxygen species (ROS), and loss of ATP production (1, 8). PT pore opening also increases the permeability of certain ions across the mitochondrial membrane, resulting in increased water influx into the matrix and consequent large-amplitude mitochondrial swelling (16, 29).

The biochemical determinants of necrotic cell death are less well defined, but similar to apoptosis, it has been suggested that the PT pore might play a major role in necrosis. PT pore

* Corresponding author. Mailing address: Manitoba Institute of Cell Biology, University of Manitoba, 100 Olivia Street, Winnipeg, MB R3E 0V9, Canada. Phone: (204) 787-2112. Fax: (204) 787-2190. E-mail: agreenb@cc.umanitoba.ca.

opening has been described in response to a rise in cytosolic free Ca^{2+}, anoxia, and reperfusion oxidative stress with overproduction of ROS in cardiac myocytes (8). Although both apoptosis and necrosis are associated with PT pore opening, necrosis is distinguished by an early loss of plasma membrane integrity and ATP, whereas both are maintained and ATP production is required for apoptosis (28, 41).

BNIP3 (formerly known as NIP3) is a member of a unique subfamily of death-inducing mitochondrial proteins that includes NIX (also called BNIP3α and BNIP3L/B5) (5, 35, 42, 61) and a *Caenorhabditis elegans* ortholog, ceBNIP3 (61; J. Cizeau and A. H. Greenberg, submitted for publication). BNIP3 family members contain a C-terminal transmembrane (TM) domain that is required for mitochondrial localization as well as for its proapoptotic activity (5, 6, 62). Many members of the BCL-2 family require a BCL-2 homology 3 (BH3) domain to induce apoptosis. BNIP3 contains a sequence that resembles a BH3 domain (amino acids 110 to 118) (61). However, in the context of the BNIP3 protein, we have shown that it is not required for heterodimerization with BCL-2 family members or cell death, both in vivo and in vitro (47), indicating that BNIP3 does not trigger apoptosis, like most BH3-containing proteins. Currently, the mechanism of induction of apoptosis and cell death by BNIP3 expression is unknown. Its localization to mitochondria, similar to several other proapoptotic BCL-2 family members, raises the possibility that BNIP3 initiates apoptosis at this site.

We report that BNIP3 induces cell death following integration into the mitochondrial outer membrane with the N terminus in the cytoplasm and the C terminus in the membrane (N_{cyto}-C_{in} orientation). Cell death is caspase independent and characterized by early plasma membrane and mitochondrial damage, before the appearance of chromatin condensation or DNA fragmentation. BNIP3 induces rapid opening of the mitochondrial PT pore accompanied by $\Delta\psi m$ suppression and increased ROS production. These changes and BNIP3-induced cell death are blocked by the PT pore inhibitors cyclosporin A and bongkrekic acid. We propose that BNIP3 activates a novel caspase-independent necrosis-like cell death pathway, which is mediated through the opening of the PT pore.

MATERIALS AND METHODS

Cell lines. MCF-7 and HeLa cells were cultured in α minimal essential medium (MEM) (Gibco-BRL) supplemented with 10% fetal bovine serum (FBS) (Cansera), 1% MEM sodium pyruvate (Gibco-BRL), 1% HEPES (Gibco-BRL), and 1% L-glutamine (Gibco-BRL). Mouse embryonic fibroblasts (MEFs) deficient in Apaf-1, caspase 9, or caspase 3 were cultured as previously described (17). 293T and 293-Bcl-2 cells were cultured in Dulbecco's modified Eagle's medium (DMEM) (Gibco-BRL) supplemented with 10% FBS.

Expression plasmids. T7-tagged pcDNA3-BNIP3, T7-tagged pcDNA3-BNIP3ΔTM (6), and HA-tagged pcDNA3-BNIP3 (5) have been described previously. pcDNA3-caspase-9-His_6 and pcDNA1-p35 were gifts from Emad Alnemri (Thomas Jefferson University, Philadelphia, Pa.). pcDNA3-Apaf-1 and pFLAG-CMV-5a-tBID were provided by Xiaodong Wang (Howard Hughes Medical Institute, Dallas, Tex.) and Junying Yuan (Harvard Medical School, Boston, Mass.), respectively.

Reagents. Murine monoclonal anti-T7 antibody was purchased from Novagen (Madison, Wis.). Murine monoclonal anti-cytochrome *c* antibodies for immunoblotting (65981A) and immunofluorescence (67971A) were purchased from Pharmingen. Mouse monoclonal anti-poly(ADP-ribose) polymerase, anti-BCL-X_L, and antiactin antibodies were purchased from Alexis Biochemicals (San Diego, Calif.), Transduction Laboratories (Lexington, Ky.), and ICN Biochemicals (Montreal, Canada), respectively. Rabbit polyclonal anti-AIF was a gift from Guido Kroemer (CNRS, Paris, France). Rabbit anti-FLAG polyclonal antibody and mouse anti-HA monoclonal antibody were purchased from Zymed (South San Francisco, Calif.) and Boehringer Mannheim (Indianapolis, Ind.), respectively. Secondary antibodies, goat anti-mouse immunoglobulin G (IgG)-horseradish peroxidase, goat anti-mouse IgG-fluorescein isothiocyanate (FITC), and goat anti-rabbit IgG-FITC were all purchased from Sigma Chemical Co. (St. Louis, Mo.). Goat anti-mouse IgG-Cy3 was from Chemicon (Temecula, Calif.).

Assessment of mitochondrial protein targeting and orientation. MCF-7 and 293T cells (10^6) were transiently transfected with LipofectAmine reagent (Gibco-BRL) with 8 μg of DNA for 12 h. Mitochondria were isolated according to Goping et al. (13) with modifications. Briefly, at 4°C, thigh muscle from the mouse hind limb or transfected cells were isolated or scraped, respectively, and washed twice in 5 ml of HIM (0.2% [wt/vol] bovine serum albumin, 200 mM mannitol, 70 mM sucrose, 10 mM HEPES-KOH, 1 mM EGTA [pH 7.5]). Cells were resuspended in 2 ml of HIM and homogenized on ice three times for 3 to 10 s using a Polytron homogenizer (setting 6.5). Large cellular debris was removed from the homogenate via centrifugation at 430 × *g* for 10 min. The supernatant was diluted in HIM (minus bovine serum albumin), and mitochondria were collected by centrifugation at 5,400 × *g* for 10 min and resuspended in cMRM (250 mM sucrose, 10 mM HEPES-KOH, 1 mM ATP, 5 mM sodium succinate, 0.08 mM ADP, 2 mM K_2HPO_4 [pH 7.5]) to 1 mg of mitochondrial protein per ml and adjusted to 1 mM dithiothreitol just prior to use.

To assess the association of proteins with the mitochondrial membrane, 30 or 100 μg of mitochondria isolated from transfected cells or tissue, respectively, were pelleted and resuspended to 0.25 mg of protein per ml in freshly prepared 0.1 M Na_2CO_3 (pH 11.5) and incubated on ice for 30 min (13). Mitochondrial membranes were collected via ultracentrifugation at 100,000 × *g* for 1 h at 4°C in a Beckman Optima TLX ultracentrifuge (Beckman Instruments, Fullerton, Calif.). Association of the proteins with the mitochondrial membrane was assessed via Western blot analysis of the pellets and the lyophilized supernatants.

To determine protein orientation, 293T cells were transiently transfected with T7-tagged BNIP3 and incubated with 3 μg of trypsin (Sigma) per ml for 10 min on ice. Trypsin was inactivated with a 100-fold excess of soybean trypsin inhibitor (Sigma). Trypsin-treated mitochondria were pelleted, subjected to alkali elution, and immunoblotted with mouse monoclonal anti-BNIP3 (Ana40) or anti-T7 (Novagen) antibodies.

β-Galactosidase cell death assay. Various doses of the peptide caspase inhibitor Ac-zVAD-fmk (Enzyme System Products, Dublin, Calif.) were applied to 10^5 293T cells cotransfected, using LipofectAmine reagent (Gibco-BRL), with 0.01 μg of the reporter plasmid pcDNA3-βgal plus the indicated expression plasmids to a final amount of 0.75 μg of DNA (see Fig. 2), as adjusted with empty vector. Cells were fixed, stained, and evaluated 27 h posttransfection as described previously (38). Similar strategies were used to evaluate the expression of pcDNA1-p35 as a caspase inhibitor (1.95 μg of DNA total) and to determine the killing efficiency of BNIP3 expressed in MEF cells (1.2 μg of DNA with 0.3 μg of β-galactosidase).

Assessment of caspase activation. Lysates were collected from 293T cells, transiently transfected via the $CaPO_4$ method (44), at the indicated times. Aliquots of these lysates were run under Laemmli sodium dodecyl sulfate-polyacrylamide gel electrophoresis (SDS-PAGE) conditions and immunoblotted with mouse monoclonal anti-PARP. Results were visualized with an enhanced chemiluminescence system (Amersham Pharmacia Biotech, Amersham, U.K.). Transfected 293T cells were also assayed for caspase cleavage via colorigenic cleavage of the peptide Ac-DEVD-pNA (Biomol, Plymouth Meeting, Pa.), according to the conditions outlined by Quignon et al. (46), using 100 μM peptide. Where appropriate, samples were preincubated with 500 nM Ac-DEVD-fmk for 30 min at room temperature. Data were acquired on a Multiskan MCC/340 (Titertek) plate reader at 405 nm.

Assessment of cytochrome *c* release. Mitochondria were isolated from $CaPO_4$-transfected 293T cells using 70 strokes (tight pestle) in a 1-ml Dounce homogenizer (Wheaton) in 300 μl of CFS buffer as previously described (52). Mitochondria were resuspended in H buffer (52). Aliquots of 5 μg of protein were analyzed on Laemmli SDS–15% PAGE gels and immunoblotted with anti-cytochrome *c* monoclonal antibody. Equal loading was ensured by probing the same blot with monoclonal antiactin. Results were visualized with enhanced chemiluminescence. Cytochrome *c* release was also determined via indirect immunofluorescence of transfected MCF-7 and 293T cells. Briefly, cells grown on coverslips were costained with Cy3-conjugated mouse anti-cytochrome *c* monoclonal antibody and an appropriate tag (HA for BNIP3 and FLAG for tBID), which was visualized with FITC-conjugated goat anti-rabbit IgG. Cells were also stained with Hoechst dye to determine apoptotic nuclear morphology. No fewer than 200 cells were scored for each sample. Fluorescence was visualized and captured using a Zeiss axiophot microscope equipped with a cooled charge-coupled device camera.

DNA fragmentation assays and annexin V staining. DNA fragmentation was detected using the in situ cell death detection kit with fluorescein (Boehringer Mannheim) as per the manufacturer's recommendations in the presence or absence of 50 μM Ac-zVAD-fmk or Ac-FA-fmk. Images were captured as described earlier. No fewer than 200 nuclei were scored manually for each sample. Annexin V staining was performed exactly as described by the manufacturer (Boehringer Mannheim), and samples were analyzed via flow cytometry.

Assessment of PT pore opening by confocal imaging. Aliquots of 293T cells were grown on coverslips, and 9 to 10 h after BNIP3 or control transfections using the $CaPO_4$ method, the cells were washed with Hanks' balanced salt solution–10 mM HEPES (pH 7.2) (HH buffer) before staining with 1 μM calcein-AM ester (Molecular Probes, Eugene, Oreg.) and 5 mM $CoCl_2$ at room temperature for 15 minutes. The $CoCl_2$ was added to quench the cytoplasmic staining so only the fluorescent mitochondria were imaged (1). Cells were washed four times and resuspended in HH buffer before imaging on an Olympus

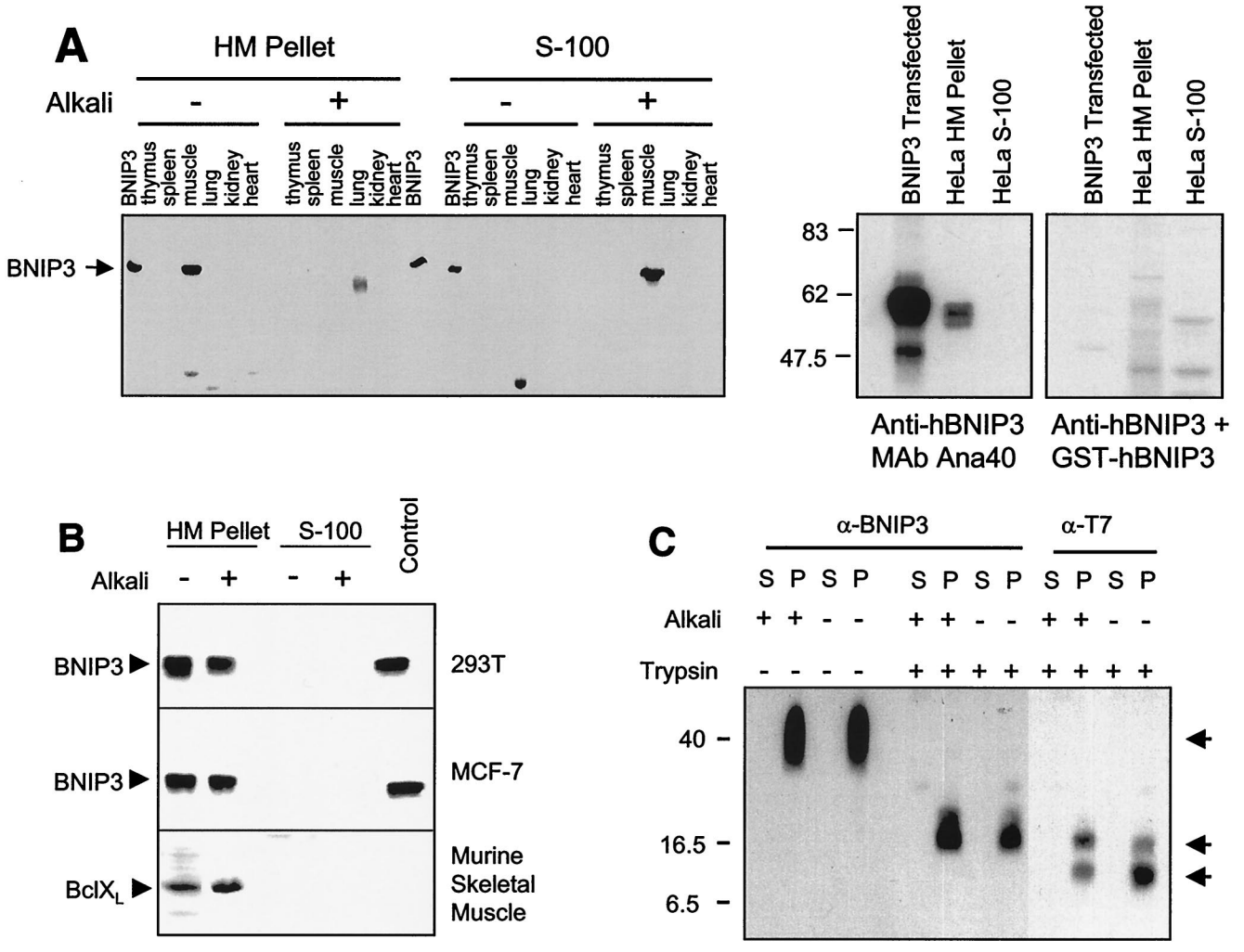

FIG. 1. BNIP3 expression and integration into the mitochondrial membrane. (A) Left panel: mitochondrion-enriched heavy membrane (HM) and S-100 cytosol (S-100) subcellular fractions of mouse tissues were isolated and alkali extracted as described in Materials and Methods, then Western blotted with polyclonal anti-BNIP3 antibody. BNIP3 lanes are lysates of 293T cells transfected with BNIP3. Right panel: HeLa cells were fractionated as described above, and fractions were Western blotted with monoclonal anti-BNIP3 antibody Ana40. Nonspecific staining was evaluated by adding GST-hBNIP3 to a parallel incubation mixture. (B) Subcellular fractions of hBNIP3-T7-transfected 293T (top) and MCF-7 (middle) cells were alkali extracted and blotted with mouse monoclonal anti-BNIP3 Ana40 antibody. Mouse skeletal muscle tissue prepared in the same manner was blotted for BCL-X_L (bottom). (C) Mitochondrial heavy membrane fractions from hBNIP3-T7-transfected 293T cells were trypsin digested and/or alkali extracted, as described in Materials and Methods, and blotted with either Ana40 mouse monoclonal anti-hBNIP3 or anti-T7 antibodies. Arrows indicate specific antibody-reactive bands at 40, 18, and 8 kDa. P, heavy membrane pellet; S, S-100 supernatant.

IX70 inverted confocal laser microscope using Fluoview 2.0 software (Carson Group Inc., Markham, Ontario, Canada). A bandpass filter of 488 nm was used for capturing the calcein images, while Nomarski optics were used to obtain transmitted light images of the cells. To determine the mitochondrial calcein fluorescence levels, individual cells were identified using Nomarski optics and total mitochondrial fluorescence per cell was measured using Northern Eclipse software, version 5.0 (Empix Inc., Toronto, Ontario, Canada).

Mitochondrial $\Delta\psi$m and ROS production. Changes in mitochondrial function were determined by incubating 10^6 293T cells, transiently transfected via the $CaPO_4$ method, with either 1 μM JC-1, 40 nM $DiOC_6$, or 2 μM dihydroethidium (HE) (all from Molecular Probes, Inc.) for 30 minutes at 37°C in Hanks' balanced salt solution (Gibco-BRL). Cells were scored using a FACScalibur flow cytometer (Becton-Dickinson, San Jose, Calif.), and data were analyzed on Cellquest software, version 3.1 (Becton-Dickinson). Controls were performed in the presence or absence of 50 μM mCICCP (Sigma) or an excess of 30% H_2O_2. For inhibition experiments, cyclosporin A (Sigma) or bongkrekic acid (a gift from J. A. Duine, Delft University, Delft, The Netherlands) was added 2 h prior to transfection. All cells were harvested 8 h after transfection and stained with 40 nM $DiOC_6$, 2 μM HE, or 1 μg of propidium iodide (PI) (Sigma) per ml. In all cases, samples were gated to exclude cellular debris.

Electron microscopy. Transfected 293T cells were fixed with 2% paraformaldehyde–0.1% gluteraldehyde in 0.1 M sodium cacodylate for 1 to 2 h at room temperature. Cells were postfixed with 1% osmium tetroxide for 1.5 h, washed, and block stained for 1 h in 3% aqueous uranyl acetate. The samples were then washed again, dehydrated with graded alcohol, and embedded in Epon-Araldyte resin (Maynard Scientific). Ultrathin sections were cut on a Reichert ultramicrotome, counterstained with 0.3% lead citrate, and examined on a Philips EM420 electron microscope.

RESULTS

Mitochondrial membrane expression and integration of BNIP3. We developed polyclonal and monoclonal antibodies to BNIP3 to examine protein expression in tissues and cell lines. Surprisingly, high levels of protein expression were found only in postnuclear lysates of murine and human skeletal muscle but not in other tissues (e.g., thymus, spleen, lung, kidney, heart, and brain) (Fig. 1A) or in many human and murine cell lines examined (data not shown). Following subcellular fractionation, the skeletal muscle BNIP3 protein was recovered in heavy membrane fractions enriched for mitochondria but not in the S-100 cytosol (Fig. 1A, left panel). Subsequent reexam-

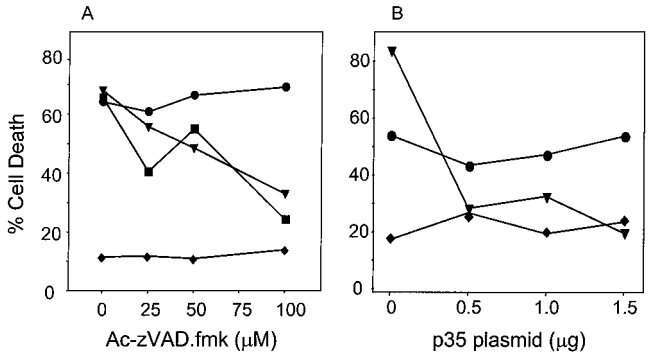

FIG. 2. Broad-spectrum caspase inhibitors Ac-zVAD-fmk and baculovirus p35 fail to inhibit BNIP3-induced cell death. (A) 293T cells were transiently cotransfected with the reporter plasmid pcDNA3-βgal and either BNIP3-T7 (●) or inactive mutant BNIP3ΔTM-T7 (◆). Cells transfected with tBID-FLAG (■) or caspase 9-His_6 plus Apaf-1 (▲) served as positive controls. All groups were treated with increasing concentrations of Ac-zVAD-fmk. (B) In a parallel experiment, 293T cells were transfected as above with increasing concentrations of pcDNA1-p35. At 27 h posttransfection, cells were fixed, stained, and evaluated for dead cells as described in Materials and Methods. The data represent one of three independent experiments with similar results.

ination of several human cell lines that had been negative in cell lysates by Western blotting revealed small amounts of BNIP3 protein in purified mitochondrial fractions using monoclonal anti-human BNIP3 (hBNIP3) Ana40. Again, no protein was detected in S-100 cytosol (Fig. 1A, right panel). The significance of these observations was unclear, as skeletal muscle is a terminally differentiated tissue and largely unaffected by programmed cell death, and the cell lines were completely viable. However, it did indicate that the endogenous BNIP3 in skeletal muscle must be inactive. Recent studies by Goping et al. (13) found that endogenous BAX is only loosely associated with the mitochondrial membrane in normal cell lines, but following death signals, it integrates fully and becomes active. We therefore examined the mitochondrial membrane association of BNIP3 in normal skeletal muscle and following transient transfection and initiation of apoptosis.

The membrane association of BNIP3 was determined following alkali extraction of mitochondria, which will dissociate and solubilize unintegrated protein. BNIP3 in mouse skeletal muscle was exclusively associated with the mitochondrion-enriched heavy membrane pellet in normal buffers (Fig. 1A), but following alkali treatment, the majority of the protein was soluble and detected in the S-100 supernatant. In contrast, endogenous $BCL\text{-}X_L$ from murine muscle remained tightly associated with the heavy membrane fractions following alkali treatment, as expected of an integral membrane protein (Fig. 1B, lower panel). We performed a similar experiment using mitochondria derived from 293T or MCF-7 cells transiently transfected with BNIP3. In contrast to the endogenous protein, transfected BNIP3 remained tightly associated with the heavy membrane fractions following alkali elution (Fig. 1B).

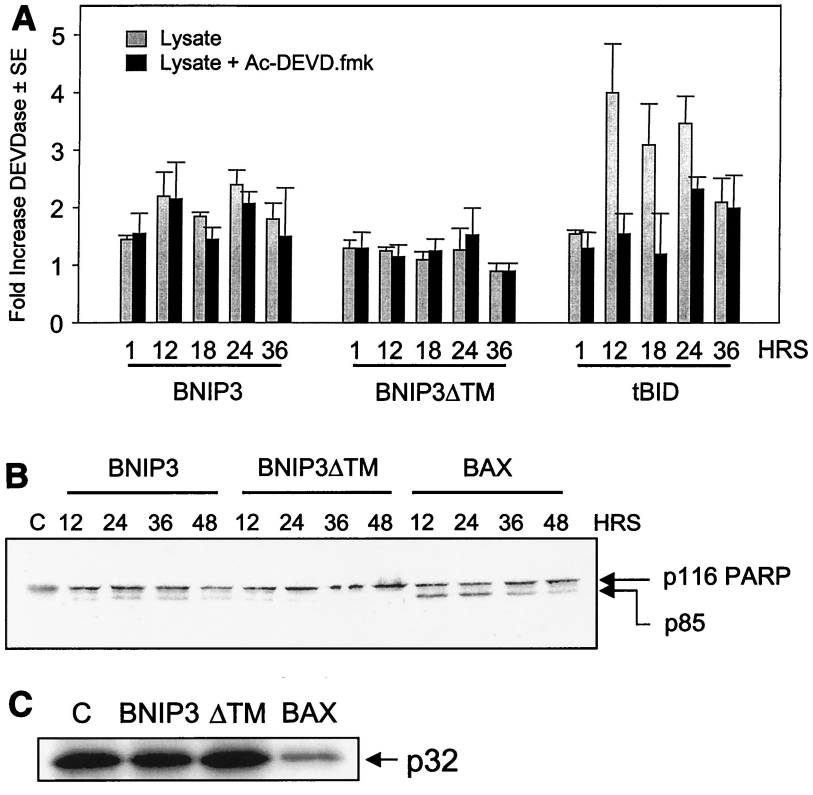

FIG. 3. BNIP3 does not activate caspases. (A) BNIP3 expression does not activate a DEVDase. Lysates from 293T cells transfected with BNIP3-T7, BNIP3ΔTM-T7, or tBID-FLAG were harvested at 1, 12, 18, 24, and 36 h and then incubated with the substrate DEVD-pNA in the presence (solid bars) or absence (shaded bars) of 500 nM Ac-DEVD-fmk. Fold activation was determined as the ratio of transfected cells to untransfected controls. Results are expressed as the mean ± standard error (SE) from at least three independent experiments. (B) BNIP3 expression fails to activate PARP cleavage. Lysates from BNIP3-T7-, BNIP3ΔTM-T7-, or BAX-transfected 293T cells were harvested at 12, 24, 36, and 48 h posttransfection and immunoblotted with mouse monoclonal anti-PARP antibody. Arrows indicate the unprocessed p116 and processed p85 bands. (C) BNIP3 expression fails to activate procaspase 3 processing. Lysates from BNIP3-T7-, BNIP3ΔTM-T7-, or BAX-transfected 293T cells were harvested 24 h posttransfection and immunoblotted with mouse monoclonal anti-procaspase 3 antibody. The arrow indicates the unprocessed p32 band. Lane C, untreated control.

Integrated BNIP3 has an N_{cyto}-C_{in} orientation in the mitochondrial outer membrane. The orientation of a protein in any membrane may be a contributing factor to its function and regulation (40). We exploited the trypsin cleavage sites in the BNIP3 TM domain (amino acids 164 to 184) and the epitope recognized by the monoclonal anti-BNIP3 antibody Ana40 (amino acids 112 to 124) to determine the mitochondrial membrane orientation of transfected BNIP3 bearing a C-terminal T7 tag.

There are three possible orientations for BNIP3 in the mitochondrial membrane that can be detected by this method: (i) mitochondrial inner membrane, (ii) mitochondrial outer membrane with an N_{cyto}-C_{in} orientation, or (iii) mitochondrial outer membrane with an N_{in}-C_{cyto} orientation. Integration of BNIP3 into the mitochondrial inner membrane would prevent exposure to trypsin and thus result in an undigested 40-kDa BNIP3 homodimer detectable by both Ana40 and anti-T7 antibodies. Alternatively, orientation of BNIP3 such that the C terminus is cytosolic would permit cleavage at R185 and R186, yielding a truncated BNIP3 homodimer of ~38 kDa that would be detected by Ana40 but not by anti-T7 antibody since the C-terminal T7 tag would be lost. Finally, a cytosolic N-terminal orientation would yield truncated fragments detectable by one or both antibodies. Following isolation of mitochondria from BNIP3-transfected cells and trypsin digestion, a prominent 18-kDa band was recognized by both antibodies and an 8-kDa band was detected by the anti-T7 but not the Ana40 antibody (Fig. 1C). The 8-kDa band was detected in the heavy membrane pellet fraction. Thus, the 8-kDa band would contain the extreme C-terminal T7 epitope and is likely a dimer of two 4-kDa monomeric C-terminal fragments representing approximately amino acids 154 to 194. This pattern is consistent with the integration of BNIP3 in the mitochondrial outer membrane in the N_{cyto}-C_{in} orientation.

BNIP3-induced cell death is caspase independent and does not induce cytochrome *c* release. To determine if BNIP3-induced cell death was mediated by caspases, we evaluated the effectiveness of the broad-spectrum peptide caspase inhibitor Ac-zVAD-fmk and the baculovirus antiapoptotic gene p35 in preventing BNIP3-induced cell death following transient transfection of 293T cells. BNIP3-induced cell death was unaffected by the same concentration of inhibitor that effectively suppressed either tBID or caspase 9/Apaf-1 transfectants by greater than 50% (Fig. 2A). Furthermore, p35 plasmid was similarly ineffective in abrogating BNIP3 cell death at concentrations of up to 1.5 μg, well above the 0.5 μg of p35 plasmid required to block caspase 9/Apaf-1-induced cell death (Fig. 2B).

The caspase substrate Ac-DEVD-pNA was used to detect the activation of caspase 3-like proteases in 293T cells transiently transfected with either BNIP3, tBID, or the inactive mutant BNIP3ΔTM. Cells were harvested at 1, 12, 18, 24, and 36 h posttransfection, and lysates were prepared and incubated with the substrate. Lysates from cells transfected with either BNIP3 or BNIP3ΔTM revealed only marginal increases in proteolytic activity and were not inhibited by the caspase inhibitor of the same specificity as Ac-DEVD-fmk (Fig. 3A). In contrast, tBID-transfected cells exhibited a fourfold increase in substrate cleavage, and this was blocked by treatment with Ac-DEVD-fmk (Fig. 3A). Lysates from BAX transfectants were similar to those of tBID transfectants (data not shown).

We next immunoblotted whole-cell lysates of BNIP3-expressing 293T cells collected at 12, 24, 36, and 48 h posttransfection for the caspase substrate PARP and found little evidence of proteolysis (Fig. 3B) and no processing of procaspase 3 (Fig. 3C). In contrast, efficient processing of PARP from 116 to 86 kDa (Fig. 3B) and procaspases 3 (Fig. 3C), 7, and 9 (data not shown) were detected in lysates from BAX transfectants. No processing of caspases 7 and 9 was detected in BNIP3 lysates up to 36 h (data not shown).

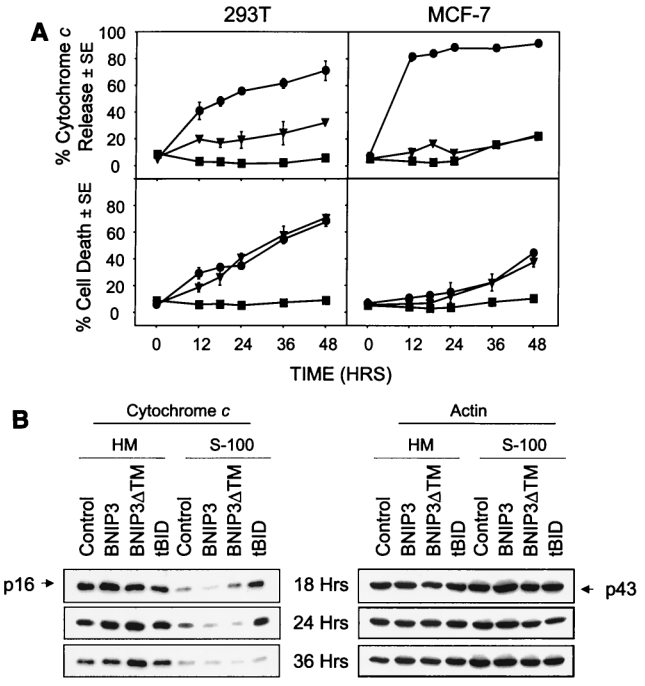

FIG. 4. BNIP3 does not induce mitochondrial cytochrome *c* release. (A) 293T cells transiently transfected with BNIP3-T7, BNIP3ΔTM-T7, or tBID-FLAG were stained with monoclonal anti-cytochrome *c* antibody and Cy3-labeled anti-mouse IgG antibody then evaluated by fluorescent microscopy. Time course of cytochrome *c* release and apoptosis following BNIP3-T7 (▼), BNIP3ΔTM-T7 (■), or tBID-FLAG (●) transfection of 293T (left panels) and MCF-7 (right panels) cells is shown. Cytochrome *c* release was scored as the loss of cytoplasmic granular staining. Apoptotic cells were scored based on chromatin condensation following Hoechst staining. The data from three independent experiments are shown as the mean ± SE for each time point. (B) Western blot analysis of the time course of release of cytochrome *c* from mitochondria into S-100 cytosol. Aliquots of 5 μg of heavy membrane (HM) and S-100 fractions from 293T cells transiently transfected with BNIP3, BNIP3ΔTM, or tBID were harvested at 18, 24, and 36 h posttransfection and Western blotted with mouse anti-cytochrome *c* antibody (p16). The same membrane was blotted with mouse antiactin antibody (p43) to demonstrate equal loading. Control, untransfected cells.

Since BNIP3 integrates into the mitochondrial outer membrane, it may act to initiate cell death by mitochondrial perturbation and the release of cytochrome *c*, a cofactor for Apaf-1. We initially used indirect immunofluorescence to examine cytochrome *c* release from cells expressing BNIP3 following transient transfection. BNIP3- and BNIP3ΔTM-expressing cells, detected by immunostaining for the C-terminal epitope tag, showed no significant cytochrome *c* release in MCF-7 cells, which are caspase 3 deficient, and only very low levels in 293T cells (Fig. 4A). On the other hand, 91% of MCF-7 and 71% of 293T cells released cytochrome *c* 48 h after transfection with tBID, while the level of cell death induced by tBID and BNIP3 was equivalent (Fig. 4A). In tBID-transfected cells, cytochrome *c* was released prior to apoptosis, as determined by Hoechst dye staining.

We next reexamined cytochrome *c* release by Western blotting heavy membrane (HM) and S-100 subcellular fractions of 293T cells at 18, 24, and 36 h posttransfection. A significant increase in cytochrome *c* was seen in the S-100 fractions of tBID but not BNIP3 transfectants at 18 and 24 h (Fig. 4B). Loss of cell viability of tBID and BNIP3 transfectants was

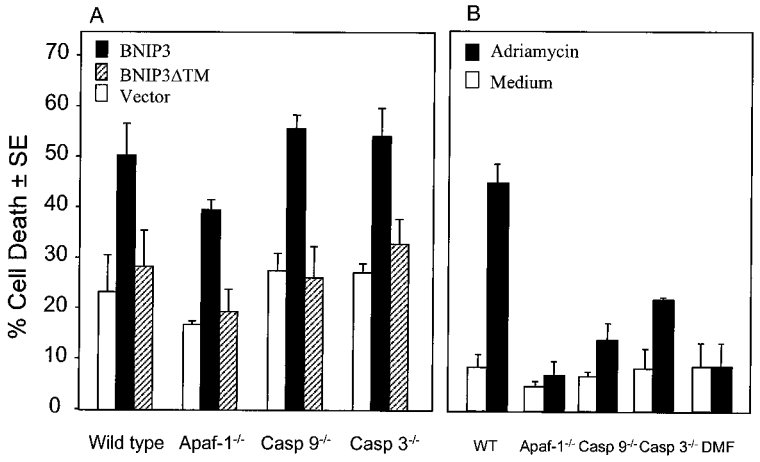

FIG. 5. BNIP3-induced cell death in the absence of Apaf-1, caspase 9, or caspase 3. (A) Wild-type, Apaf-1$^{-/-}$, caspase 9$^{-/-}$, and caspase 3$^{-/-}$ MEFs were transiently cotransfected with pcDNA3-βgal vector alone, BNIP3-T7, or BNIP3ΔTM-T7 and then scored for dead cells as described in Materials and Methods. Results are expressed as the mean ± SE from three independent experiments. (B) The same cell aliquots of wild-type (WT), Apaf-1$^{-/-}$, caspase 9$^{-/-}$ (Casp 9$^{-/-}$), and caspase 3$^{-/-}$ (Casp 3$^{-/-}$) MEFs used for the experiments in panel A were transfected with pcDNA3-βgal and treated with medium or with 3 μg of adriamycin per ml for 24 h, and dead cells were enumerated in three experiments. *N*, *N*-Dimethyl formamide (DMF) was used to dilute the adriamycin.

equivalent, as determined by trypan blue dye exclusion (data not shown). The decrease in cytochrome *c* levels in S-100 of tBID-expressing cells at 36 h was concomitant with extensive cell death. S-100 cytochrome *c* levels in BNIP3-transfected cells were similar to that of the inactive BNIP3ΔTM and control cells despite a fivefold difference in viability (Fig. 4B). A time course revealed that chromatin condensation following BNIP3 transfection preceded the release of cytochrome *c*, indicating that it could not be responsible for the nuclear changes (data not shown).

BNIP3 induces cell death in fibroblasts deficient in Apaf-1, caspase 9, or caspase 3. Since the above experiments suggested that BNIP3 induced cell death without cytochrome *c* release or caspase activation, we next examined the function of BNIP3 in cells lacking Apaf-1 or Apaf-1-activated caspases 9 and 3. Using the β-galactosidase cell death assay, wild-type, Apaf-1$^{-/-}$, caspase 9$^{-/-}$, and caspase 3$^{-/-}$ MEFs were transiently transfected with either BNIP3 or BNIP3ΔTM. BNIP3 was able to induce cell death (~50%) in the wild-type and all mutant MEF lines tested (Fig. 5A). In contrast, the mutant cells exhibited profound resistance to adriamycin-induced cell death (Fig. 5B), confirming an earlier report (17). Immunoblot analysis of whole-cell lysates showed equal expression of BNIP3 and BNIP3ΔTM in all of the MEF cell lines (data not shown).

Rapid loss of plasma membrane permeability in BNIP3-transfected cells. Cells undergoing apoptosis externalize phosphatidylserine (PS) while maintaining an intact plasma membrane (37). A time course following BNIP3 transfection identified increased plasma membrane permeability as early as 2 h posttransfection and did not increase further over the following 12 h as determined by the failure of cells to exclude PI (Fig. 6A). Cells gated to determine annexin binding as a measure of phosphatidylserine externalization in PI$^-$ populations at 12 h revealed no increase in annexin staining of BNIP3-transfected in cells that excluded PI, in contrast to cells transfected with tBID, BAX, or caspase 9/Apaf-1 (Fig. 6B). BNIP3-expressing cells analyzed at 18 and 24 h similarly did not show any increase in annexin staining in PI$^-$ cells (data not shown). Thus, BNIP3 induces early permeability of the plasma membrane but not PS externalization.

BNIP3 induces late DNA fragmentation that is independent of AIF translocation. DNA fragmentation and chromatin condensation are hallmarks of caspase-dependent apoptotic cell death and have been consistently seen in BNIP3-transfected cells (5, 6). Since we had demonstrated that plasma membrane was damaged early following BNIP3 expression, we examined the relative rate at which DNA fragmentation occurred using the TUNEL (terminal deoxynucleotidyltransferase-mediated dUTP-biotin nick end labeling) assay. BNIP3 transfectants showed increasing levels of TUNEL-positive cells over time, but no activity was detected until 18 to 24 h and maximal levels were not reached until 36 h, much slower than tBID-induced DNA damage (Fig. 7A). This contrasts with the initiation of plasma membrane damage by BNIP3 at 8 h and its completion by 18 h. In addition, we consistently observed only two or three TUNEL-positive foci in BNIP3-expressing cells, while tBID-transfected cells exhibited much more extensive nuclear fragmentation, with six to ten TUNEL-positive foci per cell (Fig. 7B). DNA fragmentation could only be partially inhibited with 50 μM Ac-zVAD-fmk in BNIP3 transfectants but was nearly completely inhibited in tBID-expressing cells (Fig. 7C). No effect was observed in parallel populations treated with 50 μM Ac-FA-fmk. We confirmed the DNA fragmentation observed

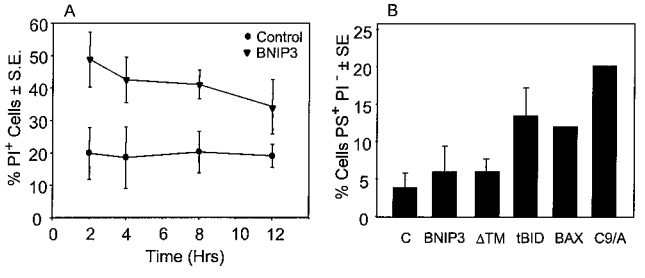

FIG. 6. BNIP3 induces rapid plasma membrane permeability but not PS externalization. (A) Untransfected and BNIP3-T7-transfected 293T cells were harvested at 2, 4, 8, and 12 h posttransfection and stained with PI. PI$^+$ cells are expressed as the mean ± SE of three or four experiments for each time point. (B) Untransfected 293T cells (C) and 293T cells transfected with BNIP3-T7 (BNIP3), BNIP3ΔTM-T7 (ΔTM), tBID-FLAG (tBID), BAX, or caspase 9/Apaf-1 (C9/A) were harvested at 12 h posttransfection and stained for annexin V and PI. Cells that were gated as PS$^+$ PI$^-$ are expressed as the mean ± SE of three independent experiments.

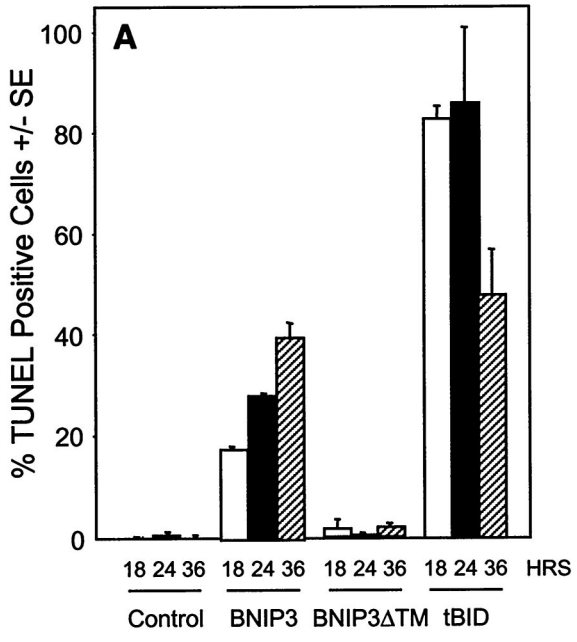

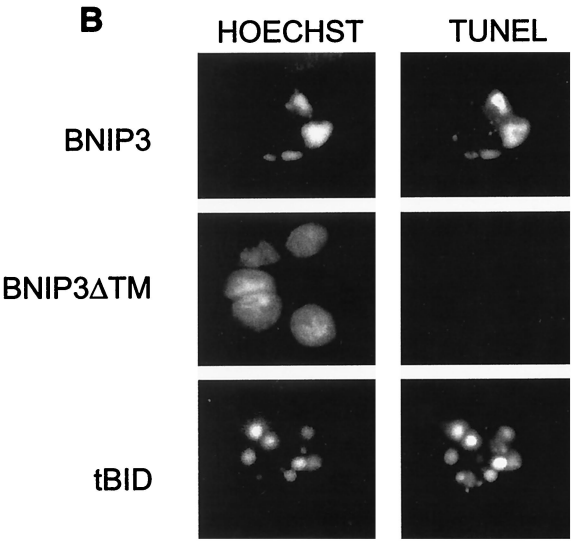

FIG. 7. BNIP3-induced cell death is characterized by late DNA fragmentation. (A) Quantification of TUNEL-positive 293T cells transiently transfected with BNIP3-T7, BNIP3ΔTM-T7, or tBID-FLAG and stained at 18, 24, and 36 h. Values for BNIP3- and tBID-transfected cells were significantly higher than those for controls at all time points ($P < 0.01$). (B) Illustration of transfected cells as in panel A harvested 24 h posttransfection and stained with the TUNEL reagent (right) or Hoechst dye (left). (C) Cells were transfected as in panel A in the absence (open bars) or presence of 50 μM Ac-FA-fmk (solid bars) or 50 μM Ac-zVAD-fmk (hatched bars). Cells were TUNEL stained 24 h posttransfection, and the percent positive was scored by fluorescent microscopy.

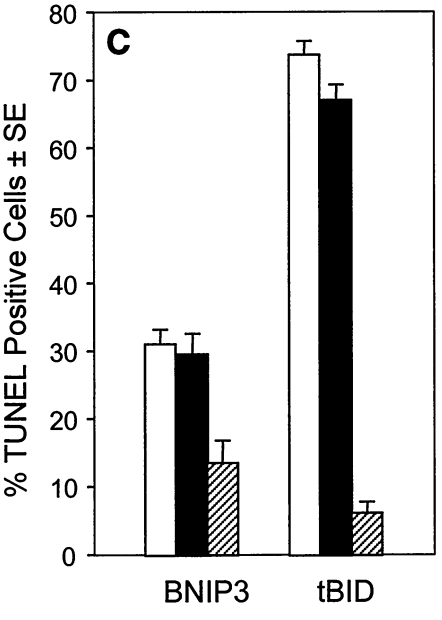

by TUNEL staining on agarose gels stained with ethidium bromide. An oligonucleosomal ladder was easily detected in tBID transfectants at 18, 24, and 36 h, while little DNA degradation and ladder formation was observed in BNIP3 transfectants even at 36 h (data not shown).

Since wild-type BNIP3-induced chromatin condensation and DNA fragmentation were not completely blocked by treatment with Ac-zVAD-fmk, we hypothesized that AIF may also mediate the BNIP3 effects. AIF is a mitochondrial flavoprotein which, in response to an apoptotic stimulus, translocates to the nucleus to induce chromatin condensation and high-molecular-weight DNA fragmentation (53). Immunofluorescence analysis and immunoblotting of heavy membrane fractions of BNIP3-transfected 293T cells at 18, 24, and 36 h posttransfection found no AIF nuclear translocation despite increases in the proportion of cells with condensed chromatin by Hoechst staining (data not shown) (C. Vande Velde, J. Cizeau, E. Daugas, G. Kroemer, and A. H. Greenberg, unpublished data).

BNIP3-expressing cells have ultrastructural features of necrosis. To determine the fine ultrastructural features of cells following BNIP3 expression, we performed transmission electron microscopy of 293T cells 24 h posttransfection. These experiments revealed a nuclear phenotype of lightly dispersed foci of chromatin condensation and heterochromatin (Fig. 8B) rather than the globular condensation typical of apoptosis. During a detailed examination of cellular organelles, we detected many rounded mitochondria in which the internal cisternae had been destroyed, while the inner and outer membranes of the mitochondria appeared to be intact in most cells (Fig. 8C). The mitochondria did not appear to be undergoing gross swelling. Surprisingly, BNIP3 transfectants were characterized by extensive cytoplasmic vacuolation and dense bodies. High-power examination of these structures revealed a heterogeneous mixture of electron-lucent and electron-dense regions, many of which appear to be vacuoles and autophagosomes (Fig. 8D and E), and some of the autophagic vacuoles contained whorls of membranous material (Fig. 8F) that have been observed during autophagic cell death (60).

BNIP3 induces mitochondrial PT pore opening, loss of Δψm, and increased ROS production. Since our studies to this point had established that BNIP3 was a mitochondrial outer membrane protein and electron micrographs of BNIP3-transfected cells featured disturbances in mitochondrial structure, we hypothesized that BNIP3 may directly induce mitochondrial dysfunction. Opening of the mitochondrial PT pore often accompanies both apoptotic and necrotic cell death, with the consequent loss of transmembrane potential (Δψm) and respiratory inhibition with ROS production. The status of the PT

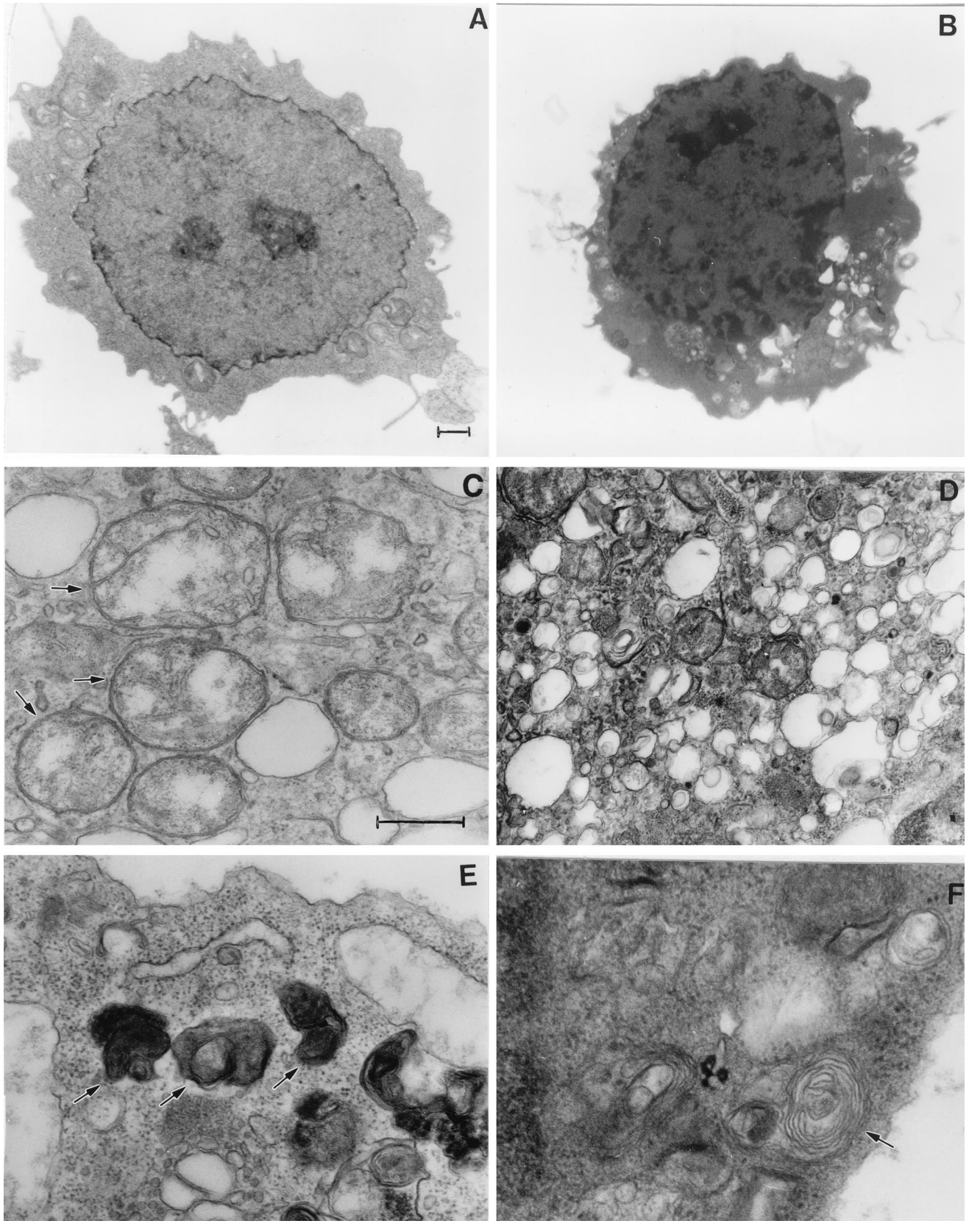

FIG. 8. BNIP3 induces ultrastructural changes of necrosis. Normal 293T cells (A) and BNIP3-expressing 293T cells (B to F) were examined 24 h posttransfection by transmission electron microscopy. Nuclei of BNIP3-expressing cells exhibited dispersed foci of chromatin condensation and heterochromatin (B) compared to control cells (A). High-power magnifications of BNIP3 transfectants showed rounded mitochondria with disrupted internal structures (arrows) (C), extensive cytoplasmic vacuolation (D), autophagosomes (arrows) (E), and autophagic vacuoles containing membranous whorls (F). (A and B), bar, 1 μm; (C to F) bar, 0.5 μm.

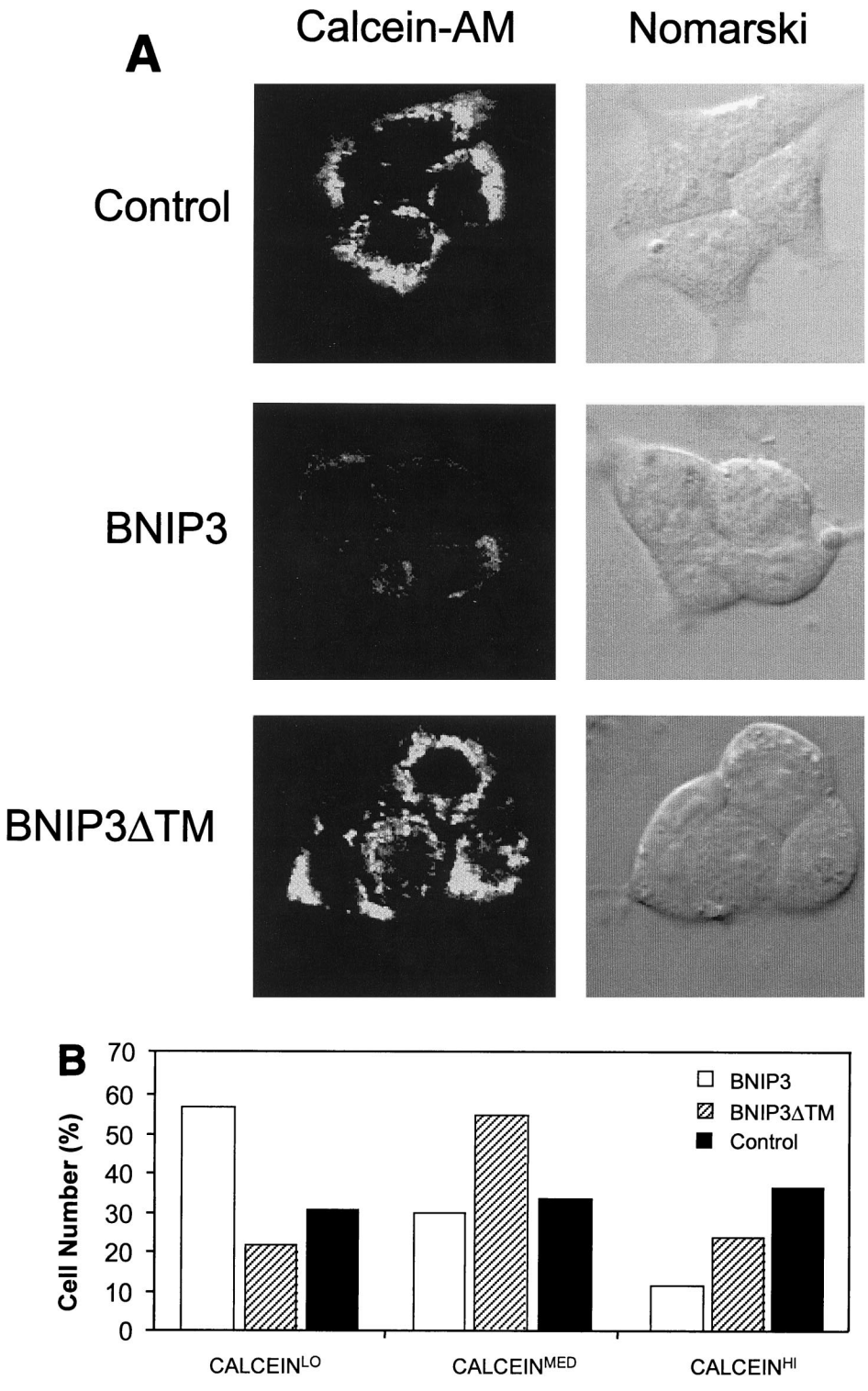

FIG. 9. BNIP3-induced cell death is characterized by mitochondrial dysfunction. (A) Untransfected (control), BNIP3-T7 (BNIP3)- and BNIP3ΔTM-T7 (BNIP3ΔTM)-transfected 293T cells were harvested 24 h after transfection and incubated with calcein-AM in the presence of $CoCl_2$ to quench cytoplasmic fluorescence. Cells were visualized by confocal laser microscopy (left) and Nomarski optics (right). (B) Quantitation of calcein fluorescence of cells transfected as described for panel A. The percentages of cells measured as low ($CALCEIN^{LO}$), intermediate ($CALCEIN^{MED}$), or high ($CALCEIN^{HI}$) total fluorescence units per cell are shown. The experiment was repeated with similar results. By chi analysis, $P < 0.001$ for the comparison of control versus BNIP3 and BNIP3ΔTM versus BNIP3. (C) Untransfected (control) and BNIP3-T7 (BNIP3)-, BNIP3ΔTM-T7 (ΔTM)-, or tBID-FLAG (tBID)-transfected 293T cells were harvested at 24 h, stained with JC-1, and analyzed by flow cytometry as a measure of $\Delta\psi m$. JC-1^{LO} cells were defined as cells that were gated within the same range as those treated with 50 μM ClCCP (~99%). BNIP3- and tBID- but not BNIP3ΔTM-transfected cells were significantly suppressed compared to controls ($P < 0.01$). (D) Cells treated as in panel C were stained with HE to measure ROS production. HE^{HI} cells were defined as cells that were gated within the same range as those treated with 30% H_2O_2 for 15 min (~98%). Levels in BNIP3- and tBID-expressing cells were significantly increased compared to untreated controls or BNIP3ΔTM ($P < 0.03$; the Student t test). (E) Samples from the control and each of the transfections in panel C were trypan blue stained as a measure of cell death. BNIP3- and tBID-transfected cells were significantly increased compared to untreated controls or BNIP3ΔTM ($P < 0.01$; the Student t test).

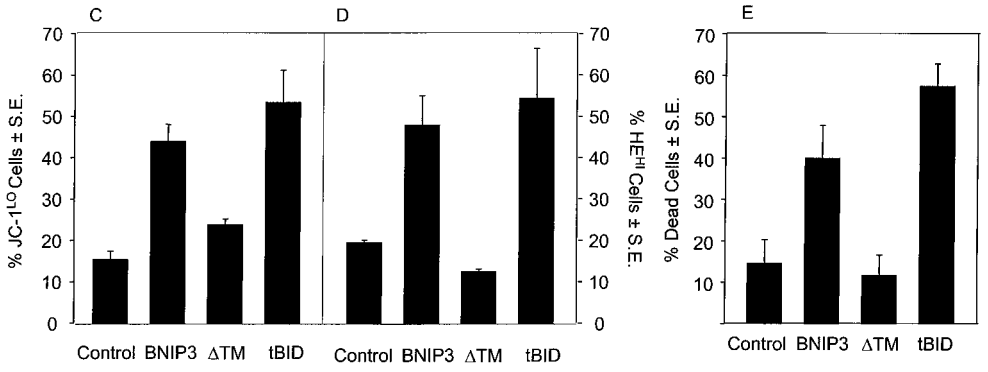

FIG. 9—*Continued.*

pore can be determined with the membrane-permeating fluorescent probe calcein-AM, which freely enters mitochondria but cannot exit except through an open PT pore following processing by cellular esterases. Using $CoCl_2$ quenching of cytosolic fluorescence as described by Bernardi et al. (1), the release of calcein from mitochondria was analyzed by confocal laser microscopy and quantitative image analysis. Following BNIP3 transfection, 293T cells lose mitochondrial calcein staining as early as 8 h posttransfection (Fig. 9A and B), indicating rapid opening of the PT pore.

To determine if BNIP3-expressing cells also decrease their transmembrane potential and produce ROS, we used the cell-permeating lipophilic dyes JC-1 and HE and assessed the staining by flow cytometry using gates established from normal untransfected 293T cells. At 24 h posttransfection, cells were collected, stained, and analyzed. BNIP3 was almost as efficient as tBID at suppressing $\Delta\psi m$, increasing ROS generation, and inducing cell death (Fig. 9C to E). These changes were identified as early as 2 h posttransfection and did not increase further during 12 h of analysis (data not shown), indicating that the mitochondrial dysfunction was maximal and occurred as early as plasma membrane permeability and cell death (Fig. 6A).

Inhibition of PT pore opening prevents mitochondrial dysfunction and cell death. To confirm that the loss of $\Delta\psi m$, increase in ROS production, and the ensuing cell death were the result of opening of the PT pore, we next examined the effect of PT pore inhibitors on BNIP3-induced cell death and mitochondrial deregulation using the potentiometric fluorescent probe $DiOC_6$ in combination with HE. BNIP3-expressing cells showed ~55% $DiOC_6$-low and HE-high cells as detected in the upper left quadrant of Fig. 10D, consistent with previous experiments using JC-1, while BNIP3ΔTM-transfected cells were not affected compared to untreated controls. As noted earlier, opening of the PT pore can be inhibited by cyclosporin A, which interacts with cyclophilin D, or bongkrekic acid, which binds to the ANT. Treatment of BNIP3 transfectants with either cyclosporin A or bongkrekic acid revealed a dose-dependent reversal in $\Delta\psi m$ suppression, ROS generation, and cell death (PI staining) (Fig. 10A to D). Maximum suppression was about 50% of that in control cells. Cells were treated with the drugs for 2 h and washed prior to transfection, a procedure that did not affect BNIP3 expression in the 293T cells (Fig. 10E). Addition of either drug during the transfection suppressed BNIP3 expression. The drugs did not affect mitochondrial function and cell death when added after the transfection.

BNIP3 physically interacts with Bcl-2 (3, 6), and Bcl-2 and Bcl-X_L overexpression can partly suppress BNIP3-induced apoptosis, although this is overcome at high BNIP3 expression levels (5, 6). We next examined the effect of Bcl-2 on BNIP3-induced cell death as measured by PI staining and found a reduction in plasma membrane damage in Bcl-2-expressing cells (Fig. 10F).

DISCUSSION

In the present study, we have determined that BNIP3 is capable of activating a novel form of cell death resembling necrosis as a consequence of mitochondrial PT pore opening. This mechanism is independent of caspases and the Apaf-1/cytochrome *c* mitochondrial pathway and occurs before the appearance of nuclear damage.

The mitochondrial membrane integration of many proapoptotic BCL-2 family members induces mitochondrial dysfunction, which plays an important role in the cell death pathway. One of the key events in apoptosis is the release of cytochrome *c*, which functions with dATP as a cofactor for Apaf-1 activation of the caspase cascade (14). There are currently three proposed models to explain the mechanism of cytochrome *c* release: (i) PT pore-induced mitochondrial swelling and subsequent outer membrane rupture (56); (ii) cytochrome *c* exit from the mitochondria through the PT pore (50); and (iii) an undefined cytochrome *c*-specific channel in the mitochondrial outer membrane (24). In one model, the PT pore is hypothesized to serve as a conduit for cytochrome *c* release into the cytoplasm. This is supported by experiments that show a direct interaction between BAX and components of the PT pore, including ANT (33) and VDAC/porin (39), and evidence that BAX may open the pore sufficiently to allow cytochrome *c* release (50). In contrast to BAX, BNIP3 does not induce cytochrome *c* release despite evidence of rapid PT pore opening. Therefore, a model in which opening of the PT pore is sufficient to release cytochrome *c* is not supported by our data. BAX must have other effects on mitochondrial membrane proteins to account for the difference with BNIP3. We do not yet know if BNIP3 interacts with the same mitochondrial pore proteins as BAX, such as ANT (33) and VDAC/porin (39). Although BNIP3 kills without cytochrome *c* release, it has been observed that the BNIP3 homolog NIX/BNIP3L/BNIP3α/B5 recombinant protein induces cytochrome *c* release from isolated mitochondria (20). The reason for this difference from BNIP3 is not known, but there are clear structural differences between the proteins that may account for this effect. In addition, because the assay was done in vitro, it will need to be confirmed that overexpression of the NIX protein induces similar effects in vivo.

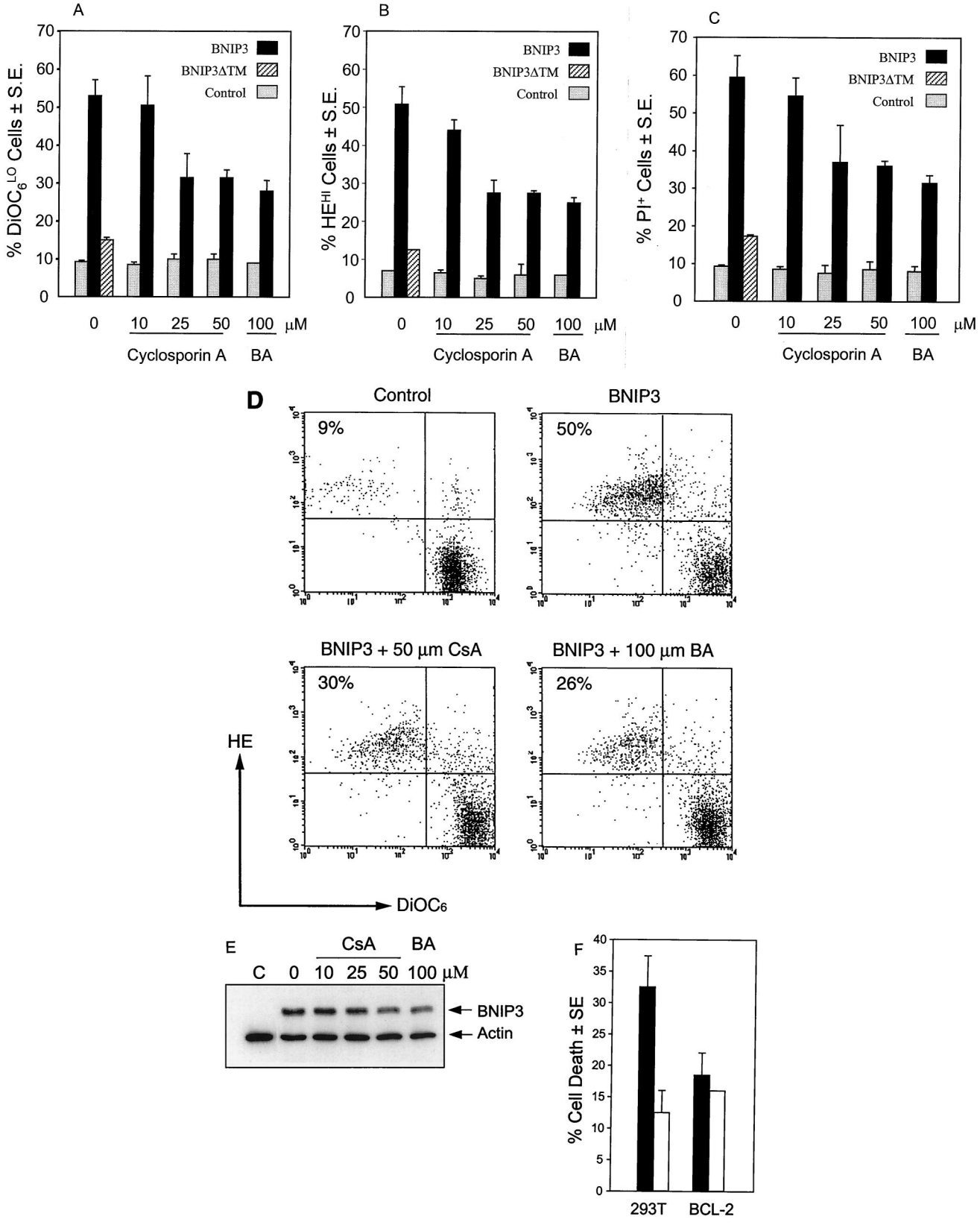

FIG. 10. Inhibition of BNIP3-induced mitochondrial dysfunction and cell death by PT pore inhibitors and Bcl-2. Untransfected (control) and BNIP3-T7-transfected 293T cells harvested 8 h posttransfection were treated with increasing doses of cyclosporin A or 100 μM bongkrekic acid (BA) and stained with $DiOC_6$ (A), HE (B), or PI (C) as described above. BNIP3ΔTM-T7-transfected 293T cells were used as a negative transfection control. Results are expressed as the mean ± SE for at least three independent experiments. (D) Flow cytometric histograms of HE and $DiOC_6$ staining of BNIP3-transfected cells treated with 50 μM cyclosporin A (CsA) or 100

Another mechanism for cytochrome *c* release occurs as a result of nonselective PT pore-induced mitochondrial matrix swelling and outer membrane rupture (56). Although electron micrographs of BNIP3-transfected 293T cells show mitochondrial rounding and destruction of cristae, we do not observe the large-amplitude swelling seen during growth factor withdrawal in interleukin-3-dependent FL5.12 cells or Fas-treated Jurkat cells (56). We have shown that cytochrome *c* release and PT pore opening can be completely separated during BNIP3-induced cell death and thus are independent events in the cell death program.

The absence of mitochondrial cytochrome *c* release does not exclude the activation of a caspase-dependent apoptotic pathway. For example, two different death pathways have been described in Fas-induced apoptosis, one of which leads to direct activation of caspase 3 through receptor-activated caspase 8 and does not require cytochrome *c*, and a second that requires mitochondrial release of cytochrome *c* to activate caspase 3 and apoptosis (49). BNIP3, on the other hand, requires neither Apaf-1/cytochrome *c* nor the downstream caspases, as BNIP3-induced cell death was unaffected by broad-spectrum caspase inhibitors and was fully functional in MEF cell lines deficient in Apaf-1, caspase 9, or caspase 3. Thus, BNIP3-induced cell death is primarily caspase independent. Induction of caspase-independent cell death has been increasingly observed, and examples include the adenoviral protein E4ORF4 (27) and cellular proteins PML (46), anti-CD2 (10), oncogenic Ras (7), and FADD (21). Furthermore, BAX and BAK are able to induce cell death, as opposed to the nuclear changes of apoptosis, in the presence of the general caspase inhibitor Ac-zVAD-fmk (36, 59). Although cell death may be caspase independent, DNA fragmentation and chromatin condensation following most apoptotic signals require downstream caspases (11). Nuclei in BNIP3 transfectants exhibit DNA fragmentation and focal chromatin condensation, although these nuclear changes are preceded by loss of plasma membrane integrity, and thus the cells are likely already committed to die. Nevertheless, it is unclear how the nuclear changes are mediated, as there is only minimal DEVDase activation, even at the late time points. Furthermore, DNA fragmentation is only partially inhibited by Ac-zVAD-fmk Immunofluorescence and immunoblotting of subcellular fractions exclude the participation of AIF, a caspase-independent mediator (53), as it was not translocated from the mitochondria to the nucleus in BNIP3-transfected cells. Ultrastructural analysis of BNIP3-transfected cells revealed that the nuclei have a peculiar mottled appearance, with dispersed foci of chromatin condensation rather than the global large-scale condensation normally observed in caspase-dependent apoptosis. Although we have not definitively determined how BNIP3 induces DNA strand breaks, it appears that the mechanism is not mediated by one of the known apoptotic pathways. Although it is possible that the DNA fragmentation is secondary to the opening of the PT pore, the toxicity of cyclosporin A and bongkrekic acid over extended incubation times following BNIP3 transfection precluded these experiments.

BNIP3 transfectants exhibit a rapid loss in plasma membrane integrity, and this precedes the appearance of DNA fragmentation detected by TUNEL. In contrast, cells expressing tBID, BAX, and caspase 9/Apaf-1 showed both the expected apoptotic phenotype of an intact plasma membrane and PS externalization (PS^+ PI^-) as well as some cells with rapid plasma membrane disruption. This observation suggests that the primary cause of BNIP3-induced cell death is the loss of membrane integrity, which would be more typical of a necrotic type of cell death. Electron micrograph analysis of BNIP3-transfected cells supports this interpretation. The morphological changes show extensive cytoplasmic vacuolation and mitochondrial deformation with minimal nuclear damage. Similar vacuole formation has been observed in caspase-independent forms of cell death, including anti-CD2-treated cells (10), neuronal cells subjected to nerve growth factor withdrawal (60), and Ac-zVAD-fmk-treated BAX and BAK transfectants (36, 59). BNIP3-expressing cells contain a heterogeneous population of electron-dense and electron-lucent vacuoles, some of which appear to be autophagic and are very similar to the structures recently observed in sympathetic neurons after nerve growth factor withdrawal (60). In this study, autophagic degeneration and vacuole formation were blocked by treatment with an autophagy inhibitor, 3-methyladenine, but not the caspase inhibitor Ac-zVAD-fmk, and may be similar to BNIP3-induced cell death. BNIP3-mediated cell death also resembles the caspase- and Apaf-1-independent cell death in the interdigital spaces of mouse limb buds, including mottled nuclei and cytoplasmic vacuolation (4). A morphologically similar form of caspase-independent cell death has been reported in the slime mold *Dictyostelium discoideum*, which was also inhibitable by cyclosporin A (43).

Opening of the PT pore, loss of $\Delta\psi m$, and increased ROS production are important contributors to cellular destruction (63) and are early events in both apoptosis and necrosis (8, 25). PT pore opening has also been described in several models of apoptotic cell death as an amplification step that is secondary to initial caspase activation (2, 12, 34). As noted earlier, necrotic cell death is similarly characterized by rapid PT pore opening that can be inhibited by cyclosporin A, which also effectively blocks cell death (25). BNIP3-induces PT pore opening with $\Delta\psi m$ suppression and ROS production occurs concurrently with plasma membrane permeabilization and is blocked by the PT pore-specific inhibitors cyclosporin A and bongkrekic acid. Thus, PT pore opening is a pivotal event for BNIP3-induced cell death. This is summarized in Fig. 11. In earlier studies, there remains a controversy as to the sequence of mitochondrial events in cell death. Zamzami et al. (63) demonstrated that ROS were generated only after dissipation of $\Delta\psi m$ following dexamethasone treatment of splenic T cells. The loss of mitochondrial membrane potential and ROS production can be both an inducer and a consequence of PT pore opening depending on the death signal (8, 26, 65). Considering the mechanism by which BNIP3 affects the PT pore, it may interact either directly or indirectly with components of the pore, resulting in its opening. Alternatively, BNIP3 may target another protein that suppresses transmembrane potential and induces ROS production, which secondarily opens the PT

μM bongkrekic acid (BA). (E) Western blot of BNIP3-transfected cells treated as described above using anti-T7 epitope antibody. Antiactin antibody was used as a loading control. Suppression of $DiOC_6$ levels in BNIP3 cells was significantly inhibited compared to BNIP3 cells at 25 μM ($P < 0.05$) and 50 μM ($P < 0.02$) cyclosporin A and 100 μM bongkrekic acid ($P < 0.02$). Increase in HE fluorescence was inhibited at 25 μM ($P < 0.03$) and 50 μM ($P < 0.02$) cyclosporin A and 100 μM bongkrekic acid ($P < 0.02$). Cell death was significantly suppressed at 50 μM cyclosporin A ($P < 0.02$), and 100 μM bongkrekic acid ($P < 0.02$). (F) BNIP3-induced cell death (solid bars) in 293T cells and 293 cells overexpressing BCL-2 (BCL-2) compared to the inactive BNIP3ΔTM mutant (open bars). Eight hours following BNIP3 transfection, cells were stained with PI and evaluated by flow cytometry. The percent dead cells were calculated as the proportion of cells that were PI positive. Equivalent transfection efficiency was obtained in both cell lines, as detected by immunostaining.

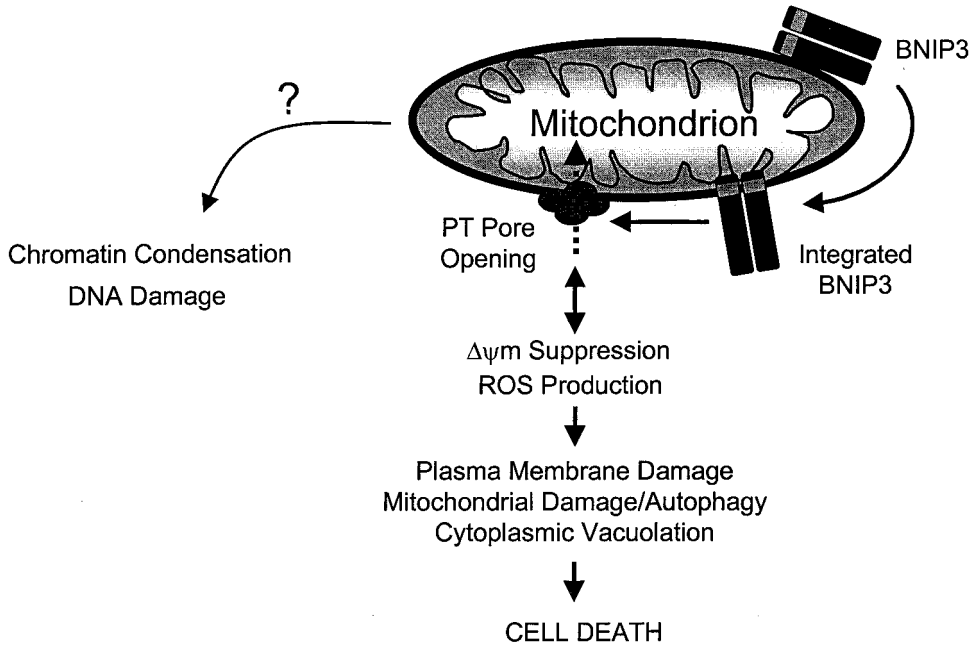

FIG. 11. Model of BNIP3-induced cell death. Overexpression permits integration of BNIP3 into the outer mitochondrial membrane in an N_{cyto}-C_{in} orientation through its TM domain. BNIP3 then initiates permeability transition pore opening and $\Delta\psi m$ suppression with increased ROS production in an undefined sequence, leading to cell death. Late DNA fragmentation and chromatin condensation are also induced as a consequence of BNIP3 integration via an unidentified pathway.

pore. Thus, although PT pore opening is a key mechanism that mediates BNIP3-induced cell death, the specific mitochondrial proteins that are targeted remain to be identified.

Based on the observed function of BNIP3 as a mediator of cell death resembling necrosis when overexpressed, it is reasonable to postulate that some forms of necrotic cell death may be mediated by endogenous BNIP3. Recently, increased endogenous BNIP3 mRNA and protein expression has been observed in HeLa cells grown in hypoxic conditions (K. Guo, G. Searfoss, C. Franks, M. Pagnoni, D. Krolikowsky, K. T. Yu, M. Jaye, K. Clark, and Y. Ivashchenko, Proceedings of the AACR Special Conference on Programmed Cell Death Regulation, abstract A-56, 2000). Hypoxia is a well-known inducer of necrotic cell death (8). Thus, it is interesting to speculate that BNIP3 may play a role in mediating death associated with hypoxic stress and possibly other forms of necrotic cell death.

Endogenous BNIP3 protein is abundant in murine and human skeletal muscle and is not detectable in lysates of all other nonskeletal muscle-bearing tissues and over 15 cell lines, including myoblasts and differentiated myocytes (D. Dubik and A. H. Greenberg, unpublished data). However, we found that some (e.g., HeLa, 293T, and K562) but not all (e.g., MCF-7) cell lines have small amounts of BNIP3 protein detectable in enriched mitochondrial fractions. Endogenous muscle BNIP3 is alkali extractable and thus loosely associated and not integrated into the mitochondrial membrane, similar to the observations for endogenous BAX intracellular localization by Goping et al. (13). When overexpressed, BNIP3 (and BAX) integrates into the mitochondrial membrane through the C-terminal transmembrane domain (amino acids 164 to 184) with the orientation of the protein in an N_{cyto}-C_{in} direction. A 17- to 18-kDa portion of the C terminus is detected after trypsin digestion of mitochondria. This would be consistent with a dimer of two trypsin-resistant fragments of 8.5 to 9.0 kDa from approximately amino acids 104 to 194. The Ana40 monoclonal reacts with amino acids 112 to 124, and this epitope is present in the trypsin-resistant fragment. The question remains how the endogenous BNIP3 remains in an inactive, nonintegrated state. At least two non-mutually exclusive mechanisms are possible: (i) endogenous BNIP3 assumes a conformation that prevents integration of the TM domain until it is altered by some posttranslational modification, or (ii) endogenous BNIP3 interacts with a regulatory protein that maintains it in an unintegrated form at the surface of the mitochondria until it dissociates. Since overexpression induces cell death, BNIP3 is able to overcome this inhibition in high concentrations, suggesting that the regulatory mechanism is saturable. Translocation from the cytoplasm to the mitochondria during induction of apoptosis has been reported for several members of the BCL-2 proapoptotic family, including BID (30, 32), BAX (13), BAK (15), BAD (9, 64), and BIM (45). These molecules can be regulated by phosphorylation, dimerization, or proteolytic cleavage (16). In the absence of an apoptotic stimulus, BAD is phosphorylated by Akt (64) and by mitochondrion-anchored protein kinase A (18) and sequestered in the cytoplasm by 14-3-3 protein (64). BAX, BAK, and BIM are held inactive in the cytoplasm and are translocated to the mitochondria after a cell death signal. Further regulation is suspected for BAX, which is permitted to integrate into the mitochondrial membrane following proteolytic cleavage of an inhibitory element in the N terminus (13). Similarly, BID is cleaved by caspase 8 following Fas ligation, resulting in mitochondrial translocation (30, 32). Whether endogenous BNIP3 translocation to the mitochondrial membrane is regulated by a posttranslational mechanism similar to these proteins remains to be determined.

In conclusion, we have shown that BNIP3 overexpression initiates a cell death pathway that is activated by protein integration into the outer mitochondrial membrane. This pathway requires PT pore opening and is independent of caspases, Apaf-1, and cytochrome *c* release. Cell death manifests as

mitochondrial dysfunction, plasma membrane damage, and the morphology of necrosis.

ACKNOWLEDGMENTS

C. Vande Velde and J. Cizeau contributed equally to this study.

We thank Peter Nickerson, Geoff Hicks, Ed Rector, and Guangming Zhong of the University of Manitoba for their assistance with flow cytometry and confocal laser microscopy, as well as Eileen MacMillan-Ward for electron microscopy preparations. We are especially grateful to Emad Alnemri, Guido Kroemer, Yuri Lazebnik, Josef Penninger, Xiaodong Wang, Junying Yuan, and J. A. Duine for their kind gift of reagents and Spencer Gibson for reviewing the manuscript and providing 293-Bcl-2 cells. We also thank Laurie Lange, Elizabeth Henson, and Angela Kemp for their excellent technical assistance and all members of the A.H.G. lab for helpful discussions.

This work was supported by the National Cancer Institute of Canada with funds from the Terry Fox Run and the Medical Research Council of Canada.

REFERENCES

1. **Bernardi, P., L. Scorrano, R. Colonna, V. Petronilli, and F. Di Lisa.** 1999. Mitochondria and cell death: mechanistic aspects and methodological issues. Eur. J. Biochem. **264:**687–701.
2. **Bossy-Wetzel, E., D. D. Newmeyer, and D. R. Green.** 1998. Mitochondrial cytochrome c release in apoptosis occurs upstream of DEVD-specific caspase activation and independently of mitochondrial transmembrane depolarization. EMBO J. **17:**37–49.
3. **Boyd, J. M., S. Malstrom, T. Subramanian, L. K. Venkatesh, U. Schaeper, B. Elangovan, C. D'Sa-Eipper, and G. Chinnadurai.** 1994. Adenovirus E1B 19 kDa and Bcl-2 proteins interact with a common set of cellular proteins. Cell **79:**341–351.
4. **Chautan, M., G. Chazal, F. Cecconi, P. Gruss, and P. Golstein.** 1999. Interdigital cell death can occur through a necrotic and caspase-independent pathway. Curr. Biol. **9:**967–970.
5. **Chen, G., J. Cizeau, C. Vande Velde, J. H. Park, G. Bozek, J. Bolton, L. Shi, D. Dubik, and A. Greenberg.** 1999. Nix and Nip3 form a subfamily of pro-apoptotic mitochondrial proteins. J. Biol. Chem. **274:**7–10.
6. **Chen, G., R. Ray, D. Dubik, L. F. Shi, J. Cizeau, R. C. Bleackley, S. Saxena, R. D. Gietz, and A. H. Greenberg.** 1997. The E1B 19K Bcl-2-binding protein Nip3 is a dimeric mitochondrial protein that activates apoptosis. J. Exp. Med. **186:**1975–1983.
7. **Chi, S., C. Kitanaka, K. Noguchi, T. Mochizuki, Y. Nagashima, M. Shirouzu, H. Fujita, M. Yoshida, W. Chen, A. Asai, M. Himeno, S. Yokoyama, and Y. Kuchino.** 1999. Oncogenic Ras triggers cell suicide through the activation of a caspase-independent cell death program in human cancer cells. Oncogene **18:**2281–2290.
8. **Crompton, M.** 1999. The mitochondrial permeability transition pore and its role in cell death. Biochem. J. **341:**233–249.
9. **Datta, S. R., H. Dudek, X. Tao, S. Masters, H. A. Fu, Y. Gotoh, and M. E. Greenberg.** 1997. Akt phosphorylation of BAD couples survival signals to the cell-intrinsic death machinery. Cell **91:**231–241.
10. **Deas, O., C. Dumont, M. MacFarlane, C. Rouleau, F. Hebib, F. Harper, F. Hirsch, G. M. Charpentier, G. M. Cohen, and A. Senik.** 1998. Caspase-independent cell death induced by anti-CD2 or staurosporine in activated human peripheral T lymphocytes. J. Immunol. **161:**3375–3383.
11. **Earnshaw, W. C., L. M. Martins, and S. H. Kaufmann.** 1999. Mammalian caspases: structure, activation, substrates, and functions during apoptosis. Annu. Rev. Biochem. **68:**383–424.
12. **Finucane, D. M., E. Bossy-Wetzel, N. J. Waterhouse, T. G. Cotter, and D. R. Green.** 1999. Bax-induced caspase activation and apoptosis via cytochrome c release from mitochondria is inhibitable by Bcl-xL. J. Biol. Chem. **274:**2225–2233.
13. **Goping, I. S., A. Gross, J. N. Lavoie, M. Nguyen, R. Jemmerson, K. Roth, S. J. Korsmeyer, and G. C. Shore.** 1998. Regulated targeting of BAX to mitochondria. J. Cell. Biol. **143:**207–215.
14. **Green, D. R., and J. C. Reed.** 1998. Mitochondria and apoptosis. Science **281:**1309–1312.
15. **Griffiths, G. J., L. Dubrez, C. P. Morgan, N. A. Jones, J. Whitehouse, B. M. Corfe, C. Dive, and J. A. Hickman.** 1999. Cell damage-induced conformational changes of the pro-apoptotic protein bak in vivo precede the onset of apoptosis. J. Cell Biol. **144:**903–914.
16. **Gross, A., J. M. McDonnell, and S. J. Korsmeyer.** 1999. BCL-2 family members and the mitochondria in apoptosis. Genes Dev. **13:**1899–1911.
17. **Hakem, R., A. Hakem, G. S. Duncan, J. T. Henderson, M. Woo, M. S. Soengas, A. Elia, J. L. De la Pompa, D. Kagi, W. Khoo, J. Potter, R. Yoshida, S. A. Kaufman, S. W. Lowe, J. M. Penninger, and T. W. Mak.** 1998. Differential requirement for caspase 9 in apoptotic pathways in vivo. Cell **94:**339–352.
18. **Harada, H., B. Becknell, M. Wilm, M. Mann, L. J. S. Huang, S. S. Taylor, J. D. Scott, and S. J. Korsmeyer.** 1999. Phosphorylation and inactivation of BAD by mitochondria-anchored protein kinase A. Mol. Cell **3:**413–422.
19. **Horvitz, H. R.** 1999. Genetic control of programmed cell death in the nematode Caenorhabditis elegans. Cancer Res. **59:**1701S–1706S.
20. **Imazu, T., S. Shimizu, S. Tagami, M. Matsushima, Y. Nakamura, T. Miki, A. Okuyama, and Y. Tsujimoto.** 1999. Bcl-2/E1B 19kDa-interacting protein 3-like protein (Bnip3L) interacts with Bcl-2/Bcl-xL and induces apoptosis by altering mitochondrial membrane permeability. Oncogene **18:**4523–4529.
21. **Kawahara, A., Y. Ohsawa, H. Matsumura, Y. Uchiyama, and S. Nagata.** 1998. Caspase-independent cell killing by Fas-associated protein with death domain. J. Cell Biol. **143:**1353–1360.
22. **Kerr, J. F. R., A. H. Wyllie, and A. R. Currie.** 1972. Apoptosis: a basic biological phenomenon with wide-ranging implications in tissue kinetics. Br. J. Cancer **26:**239–257.
23. **Kitanaka, C., and Y. Kuchino.** 1999. Caspase-independent programmed cell death with necrotic morphology. Cell Death Differ. **6:**508–515.
24. **Kluck, R. M., M. Degli-Esposti, G. Perkins, T. Renken, T. Kuwana, E. Bossy-Wetzel, Y. P. Goldberg, T. D. Allen, M. J. Farber, D. R. Green, and D. D. Newmeyer.** 1999. The pro-apoptotic proteins Bid and Bax cause a limited permeabilization of the mitochondrial outer membrane that is enhanced by cytosol. J. Cell. Biol. **147:**809–822.
25. **Kroemer, G., B. Dallaporta, and M. Resche-Rigon.** 1998. The mitochondrial death/life regulator in apoptosis and necrosis. Annu. Rev. Physiol. **60:**619–642.
26. **Kroemer, G., N. Zamzami, and S. A. Susin.** 1997. Mitochondrial control of apoptosis. Immunol. Today **18:**44–51.
27. **Lavoie, J. N., M. Nguyen, R. C. Marcellus, P. E. Branton, and G. C. Shore.** 1998. E4orf4, a novel adenovirus death factor that induces p53-independent apoptosis by a pathway that is not inhibited by zVAD-fmk. J. Cell Biol. **140:**637–645.
28. **Leist, M., B. Single, A. F. Castoldi, S. Kuhnle, and P. Nicotera.** 1997. Intracellular adenosine triphosphate (ATP) concentration: a switch in the decision between apoptosis and necrosis. J. Exp. Med. **185:**1481–1486.
29. **Lemasters, J. J., A. L. Nieminen, T. Qian, L. C. Trost, S. P. Elmore, Y. Nishimura, R. A. Crowe, W. E. Cascio, C. A. Bradham, D. A. Brenner, and B. Herman.** 1998. The mitochondrial permeability transition in cell death: a common mechanism in necrosis, apoptosis and autophagy. Biochim. Biophys. Acta **1366:**177–196.
30. **Li, H., H. Zhu, C. J. Xu, and J. Yuan.** 1998. Cleavage of BID by caspase 8 mediates the mitochondrial damage in the Fas pathway of apoptosis. Cell **94:**491–501.
31. **Li, P., D. Nijhawan, I. Budihardjo, S. M. Srinivasula, M. Ahmad, E. S. Alnemri, and X. D. Wang.** 1997. Cytochrome c and dATP-dependent formation of Apaf-1/caspase-9 complex initiates an apoptotic protease cascade. Cell **91:**479–489.
32. **Luo, X., I. Budihardjo, H. Zou, C. Slaughter, and X. Wang.** 1998. Bid, a Bcl2 interacting protein, mediates cytochrome c release from mitochondria in response to activation of cell surface death receptors. Cell **94:**481–490.
33. **Marzo, I., C. Brenner, N. Zamzami, J. M. Juergensmeier, S. A. Susin, H. L. A. Vieira, M. C. Prevost, Z. H. Xie, S. Matsuyama, J. C. Reed, and G. Kroemer.** 1998. Bax and adenine nucleotide translocator cooperate in the mitochondrial control of apoptosis. Science **281:**2027–2031.
34. **Marzo, I., C. Brenner, N. Zamzami, S. A. Susin, G. Beutner, D. Brdiczka, R. Remy, Z. H. Xie, J. C. Reed, and G. Kroemer.** 1998. The permeability transition pore complex: A target for apoptosis regulation by caspases and Bcl-2-related proteins. J. Exp. Med. **187:**1261–1271.
35. **Matsushima, M., T. Fujiwara, E. Takahashi, T. Minaguchi, Y. Eguchi, Y. Tsujimoto, K. Suzumori, and Y. Nakamura.** 1998. Isolation, mapping, and functional analysis of a novel human cDNA (BNIP3L) encoding a protein homologous to human Nip3. Genes Chromosomes Cancer **21:**230–235.
36. **McCarthy, N. J., M. K. B. Whyte, C. S. Gilbert, and G. I. Evan.** 1997. Inhibition of Ced-3/ICE-related proteases does not prevent cell death induced by oncogenes, DNA damage, or the Bcl-2 homologue Bak. J. Cell Biol. **136:**215–227.
37. **McConkey, D. J.** 1998. Biochemical determinants of apoptosis and necrosis. Toxicol. Lett. **99:**157–168.
38. **Miura, M., H. Zhu, R. Rotello, E. A. Hartwieg, and J. Yuan.** 1993. Induction of apoptosis in fibroblasts by IL-1beta-converting enzyme, a mammalian homolog of the C. elegans cell death gene ced−. Cell **75:**653–660.
39. **Narita, M., S. Shimizu, T. Ito, T. Chittenden, R. J. Lutz, H. Matsuda, and Y. Tsujimoto.** 1998. Bax interacts with the permeability transition pore to induce permeability transition and cytochrome c release in isolated mitochondria. Proc. Natl. Acad. Sci. USA **95:**14681–14686.
40. **Nguyen, M., D. G. Millar, V. W. Yong, S. J. Korsmeyer, and G. C. Shore.** 1993. Targeting of Bcl-2 to the mitochondrial outer membrane by a COOH-terminal signal anchor sequence. J. Biol. Chem. **268:**25265–25268.
41. **Nicotera, P., M. Leist, and E. Ferrando-May.** 1998. Intracellular ATP, a switch in the decision between apoptosis and necrosis. Toxicol. Lett. **102–103:**139–142.
42. **Ohi, N., A. Tokunaga, H. Tsunoda, K. Nakano, K. Haraguchi, K. Oda, N. Motoyama, and T. Nakajima.** 1999. A novel adenovirus E1B19K-binding

protein B5 inhibits apoptosis induced by Nip3 by forming a heterodimer through the C-terminal hydrophobic region. Cell Death Differ. **6:**314–325.
43. **Olie, R. A., F. Durrieu, S. Cornillon, J. Loughran, J. Gross, W. C. Earnshaw, and P. Golstein.** 1998. Apparent caspase independence of programmed cell death in Dictyostelium. Curr. Biol. **8:**955–958.
44. **Pear, W. S., G. P. Nolan, M. L. Scott, and D. Baltimore.** 1995. Production of high-titer helper-free retroviruses by transient transfection. Proc. Natl. Acad. Sci. USA **90:**8392–8396.
45. **Puthalakath, H., D. C. S. Huang, L. A. O'Reilly, S. M. King, and A. Strasser.** 1999. The proapoptotic activity of the Bcl-2 family member Bim is regulated by interaction with the dynein motor complex. Mol. Cell **3:**287–296.
46. **Quignon, F., F. De Bels, M. Koken, J. Feunteun, J. C. Ameisen, and H. De The.** 1998. PML induces a novel caspase-independent death process. Nat. Genet. **20:**259–265.
47. **Ray, R., G. Chen, C. Vande Velde, J. Cizeau, R. D. Gietz, J. C. Reed, and A. H. Greenberg.** 2000. BNIP3 heterodimerizes with Bcl-2/Bcl-X_L and induces cell death independent of the BH3 domain at both mitochondrial and non-mitochondrial sites. J. Biol. Chem. **275:**1439–1448.
48. **Salvesen, G. S., and V. M. Dixit.** 1999. Caspase activation: the induced-proximity model. Proc. Natl. Acad. Sci. USA **96:**10964–10967.
49. **Scaffidi, C., S. Fulda, A. Srinivasan, C. Friesen, F. Li, K. J. Tomaselli, K. M. Debatin, P. H. Krammer, and M. E. Peter.** 1998. Two CD95 (APO-1/Fas) signaling pathways. EMBO J. **17:**1675–1687.
50. **Shimizu, S., M. Narita, and Y. Tsujimoto.** 1999. Bcl-2 family proteins regulate the release of apoptogenic cytochrome c by the mitochondrial channel VDAC. Nature **399:**483–487.
51. **Srinivasula, S. M., M. Ahmad, T. Fernandes-Alnemri, and E. S. Alnemri.** 1998. Autoactivation of procaspase-9 by Apaf-1-mediated oligomerization. Mol. Cell **1:**949–957.
52. **Susin, S. A., N. Larochette, M. Geuskens, and G. Kroemer.** 2000. Purification of mitochondria for apoptosis assays. Methods Enzymol., in press.
53. **Susin, S. A., H. K. Lorenzo, N. Zamzami, I. Marzo, B. E. Snow, G. M. Brothers, J. Mangion, E. Jacotot, P. Costantini, M. Loeffler, N. Larochette, D. R. Goodlett, R. Aebersold, D. P. Siderovski, J. M. Penninger, and G. Kroemer.** 1999. Molecular characterization of mitochondrial apoptosis-inducing factor. Nature **397:**441–446.
54. **Thornberry, N. A., and Y. Lazebnik.** 1998. Caspases: enemies within. Science **281:**1312–1316.
55. **Tsujimoto, Y.** 1997. Apoptosis and necrosis: intracellular ATP level as a determinant for cell death modes. Cell Death Differ. **4:**429–434.
56. **Vander Heiden, M. G., N. S. Chandel, E. K. Williamson, P. T. Schumacker, and C. B. Thompson.** 1997. Bcl-xL regulates the membrane potential and volume homeostasis of mitochondria. Cell **91:**627–637.
57. **Vaux, D. L., and S. J. Korsmeyer.** 1999. Cell death in development. Cell **96:**245–254.
58. **Wyllie, A. H., F. F. R. Kerr, and A. R. Currie.** 1980. Cell death: the significance of apoptosis. Int. Rev. Cytol. **68:**251–305.
59. **Xiang, J. L., D. T. Chao, and S. J. Korsmeyer.** 1996. BAX-induced cell death may not require interleukin 1beta-converting enzyme-like proteases. Proc. Natl. Acad. Sci. USA **93:**14559–14563.
60. **Xue, L. Z., G. C. Fletcher, and A. M. Tolkovsky.** 1999. Autophagy is activated by apoptotic signalling in sympathetic neurons: an alternative mechanism of death execution. Mol. Cell Neurosci. **14:**180–198.
61. **Yasuda, M., J. W. Han, C. A. Dionne, J. M. Boyd, and G. Chinnadurai.** 1999. BNIP3alpha: a human homolog of mitochondrial proapoptotic protein BNIP3. Cancer Res. **59:**533–537.
62. **Yasuda, M., P. Theodorakis, T. Subramanian, and G. Chinnadurai.** 1998. Adenovirus E1B-19K/BCL-2 interacting protein BNIP3 contains a BH3 domain and a mitochondrial targeting sequence. J. Biol. Chem. **273:**12415–12421.
63. **Zamzami, N., P. Marchetti, M. Castedo, D. Decaudin, A. Macho, T. Hirsch, S. A. Susin, P. X. Petit, B. Mignotte, and G. Kroemer.** 1995. Sequential reduction of mitochondrial transmembrane potential and generation of reactive oxygen species in early programmed cell death. J. Exp. Med. **182:**367–377.
64. **Zha, J. P., H. Harada, E. Yang, J. Jockel, and S. J. Korsmeyer.** 1996. Serine phosphorylation of death agonist BAD in response to survival factor results in binding to 14-3-3 not BGL-XL. Cell **87:**619–628.
65. **Zoratti, M., and I. Szabo.** 1995. The mitochondrial permeability transition. Biochim. Biophys. Acta **1241:**139–176.